Research Article Vol. 10, No. 10 / October 2023 / Optica 1353

OPTICA

Near-unity excess noise factor of staircase avalanche photodiodes

Adam A. Dadey,[1] Andrew H. Jones,[1] Stephen D. March,[2] Seth R. Bank,[2] and Joe C. Campbell[1,*]

[1]Department of Electrical and Computer Engineering, University of Virginia, Charlottesville, Virginia 22903, USA
[2]Department of Electrical and Computer Engineering, University of Texas at Austin, Austin, Texas 78758, USA
*jcc7s@virginia.edu

Received 26 May 2023; revised 7 September 2023; accepted 14 September 2023; published 12 October 2023

If a receiver system is circuit-noise limited, avalanche photodiodes can be beneficial, as their internal gain mechanism can lead to a higher system signal-to-noise ratio. However, the extent of this benefit is intrinsically limited by the detectors' excess noise factor. The higher the factor, the lower the overall signal-to-noise ratio. The staircase avalanche photodiode proposed by Federico Capasso was designed to be a solid-state replacement for a photomultiplier tube in which discrete and deterministic gain would lead to a unity excess noise factor. The predicted gains for a staircase avalanche photodiode have recently been confirmed for one-, two-, and three-step structures [Nat. Photonics 15, 468 (2021)]. This paper presents measurements of the excess noise factor of two- and three-step staircase avalanche photodiodes. At an average gain of 4.01 and 7.24, the two- and three-step staircase avalanche photodiodes have an average excess noise factor of 1.02 and 1.08, respectively.

https://doi.org/10.1364/OPTICA.496587

1. INTRODUCTION

The most common sources of noise in an optical receiver are dark current and thermal noise in the detector, circuit noise in the electronics that follow the detector, or the quantum noise in the signal. Quantum noise is not an issue for most applications. Dark current issues are usually addressed by materials studies or cooling to reduce bulk sources and by developing passivation techniques to suppress surface leakage. If circuit noise is the limiting mechanism, using a detector with internal gain, such as a photomultiplier tube (PMT) or an avalanche photodiode (APD), is beneficial. The advantages and disadvantages of PMTs are well documented. Their high gain, low noise, and large active area are offset in many applications by their cost, size, fragility, limited response in the infrared, and high bias voltage. APDs are complementary to PMTs in that they can be designed to operate over a broad spectral range, require lower bias voltages, cost less, operate at higher speeds, and are more robust. However, conventional APDs exhibit higher multiplication-related noise, and the active area diameter is typically tens of microns. The multiplication noise in a conventional APD happens because impact ionization is a random process, which results in a variation in the gain from one injected carrier to the next. The mean squared noise current density of both types of detectors can be expressed as

$$S = 2q(I_{\text{photo}} + I_{\text{dark}})\langle M\rangle^2 F(M), \tag{1}$$

where q is the elementary charge, I_{photo} and I_{dark} are the unity gain ($\langle M\rangle = 1$) photocurrent and dark current, and $\langle M\rangle$ is the average value of the gain. The excess noise factor, $F(M)$, is defined as the normalized second moment of the gain random variable for a single input photocarrier, i.e., $F(M) = \langle M^2\rangle/\langle M\rangle^2$ accounts for variation or randomness of the gain. The excess noise factor can also be expressed in terms of the mean and variance of the gain by $F(M) = 1 + \text{var}(M)/\langle M\rangle^2$. For deterministic gain, which is characteristic of PMTs, $\text{var}(M) = 0$. For conventional APDs, however, this is not the case, which results in overall higher noise performance and reduced signal-to-noise ratio (SNR).

There have been many attempts to develop solid-state photodetectors in which the gain is as deterministic as PMTs, with concomitant low noise. One of the more intriguing approaches, the staircase APD, was proposed in the early 1980s by Capasso and co-workers [1]. The staircase APD structure consists of sequential bandgap graded regions [Fig. 1(a)], which, under reverse bias, create a series of steps, as shown in Fig. 1(b).

Electrons that move from the wide to narrow bandgap regions acquire excess energy, which enables immediate, localized impact ionization. These discontinuities are somewhat analogous to dynodes in a photomultiplier, creating a more deterministic gain process with a resultant reduction in gain fluctuations and, thus, lower excess noise. Ideally, the probability of impact ionization is unity at each step, generating a gain of 2^n where n is the number of steps [1]. If the probability for impact ionization is less than one and differs for each step, the gain is characterized by a shifted Bernoulli distribution. The gain is given by the expression

$$\langle M\rangle = \prod_{i=1}^{n}\langle\gamma_i\rangle, \tag{2}$$

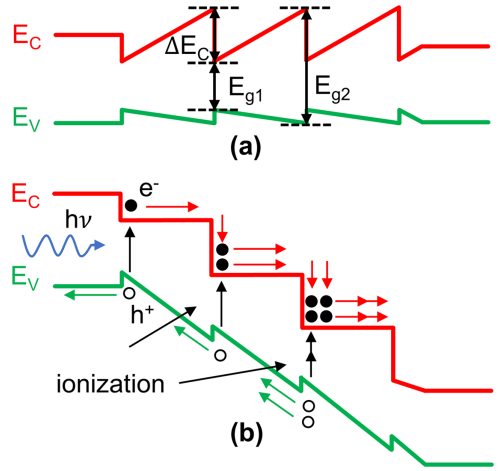

Fig. 1. (a) Energy band diagram of unbiased staircase APD. (b) Illustration of localized impact ionization under reverse bias.

where $\langle \gamma_i \rangle$ is the mean gain at the i_{th} staircase step. Bernoulli statistics represent the probability distribution for impact ionization at each step. If all the carriers crossing a step impact ionize, $\langle \gamma_i \rangle = 2$. Conversely, if no ionizations occur, $\langle \gamma_i \rangle = 1$. Initially, Capasso *et al*. used $Al_xGa_{1-x}As/GaAs$ to fabricate the staircase band structures [2,3]. Unfortunately, the $Al_xGa_{1-x}As/GaAs$ conduction band discontinuity is insufficient to allow carriers to impact ionize in GaAs, particularly for high-energy electrons scattered to satellite valleys [4]. The $Al_xIn_{1-x}As_ySb_{1-y}$ material system, however, is well suited for the staircase APD structure. The direct bandgap is widely tunable from 0.24 eV ($x = 0$) to 1.25 eV ($x = 0.8$) [5], and the change in bandgap occurs almost entirely in the conduction band [6]. March *et al*., using one-, two-, and three-step AlInAsSb staircase structures, have successfully demonstrated 2^n gain scaling [7]. This paper reports measurements of the excess noise factor for two- and three-step staircase APDs.

The staircase APD wafers were grown as digital alloys of the binaries AlSb, AlAs, AlSb, and InSb on n-type GaSb (001) substrates. Details of the crystal growth and properties of the resulting materials are reported elsewhere [5,6,8,9]. Figure 2 shows the epitaxial layer structure of the staircase APD and a corresponding control structure where the staircase region has been replaced with $Al_{0.7}InAsSb$, allowing for staircase performance to be directly compared to a simple homojunction. This control structure was grown in the same batch as the complementary staircase APD, back-to-back, and it is used to calculate its gain as detailed in a previous publication [7]. Circular mesas were defined by standard photolithography and formed by etching the mesas into the n-type $Al_{0.7}InAsSb$ contact layer with a citric/phosphoric acid solution. The devices were passivated with SU-8 to reduce surface leakage current. Ti/Au contacts were deposited using electron-beam evaporation.

2. THEORETICAL EXCESS NOISE FOR STAIRCASE APDs

Theories for the gain and excess noise factor for staircase APDs are well documented [1,10–12]. The excess noise factor for an n-step staircase APD in which a single carrier can initiate a single impact ionization at each discontinuity in the band structure is given by the expression [10,12]

$$F = 1 + \frac{\text{var}(\gamma_1)}{\langle \gamma_1 \rangle^2} + \sum_{i=2}^{n} \left[\frac{\text{var}(\gamma_i)}{\langle \gamma_i \rangle^2 \prod_{k=1}^{i-1} \langle \gamma_k \rangle} \right], \tag{3}$$

where $\text{var}(\gamma_i)$ is the variance of the multiplication at the i_{th} step. This equation is valid for staircase APDs with a different gain value at each step. Since it is difficult to determine the impact ionization probabilities for individual steps, we estimate the excess noise factor, assuming the probabilities are the same at each step. Under this assumption, the excess noise factor becomes [1,10–12]

$$F = 1 + \frac{\text{var}(\gamma)}{\langle \gamma \rangle (\langle \gamma \rangle - 1)} \left[1 - \frac{1}{\langle \gamma^n \rangle} \right]. \tag{4}$$

For staircase APDs, Teich *et al*. [10] have shown that $\langle \gamma \rangle = 1 + P$ and $\text{var}(\gamma) = P(1 - P)$, as expected from Bernoulli statistics. Using these expressions, Eq. (4) can be rewritten as

$$F = 1 + \frac{1 - P}{1 + P} \left[1 - \frac{1}{(1 + P)^n} \right]. \tag{5}$$

For the two-step staircase, the measured gain at −2.5 V bias is 4.01, which gives calculated values of ∼1 for P and $F = 1.00$. The three-step APD exhibited a gain of 7.24 at −4 V bias. The corresponding values of P and F are 0.93 and 1.03, respectively.

3. EXCESS NOISE MEASUREMENT SETUP

The noise for the two- and three-step staircase APD devices was measured at a low frequency of around 70 kHz to ensure the devices were not bandwidth-limited. Figure 3 shows a block diagram of the

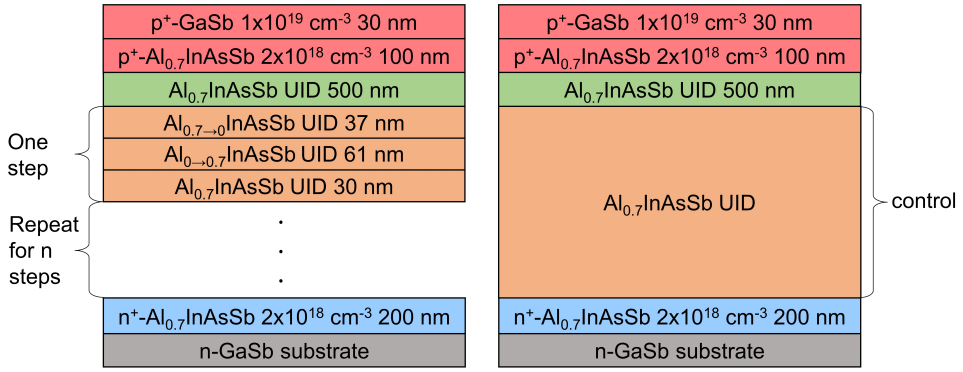

Fig. 2. Epitaxial layer structure for an n-step staircase APD (left) and the epitaxial layer structure for a corresponding control structure where the staircase step region has been replaced with $Al_{0.7}InAsSb$.

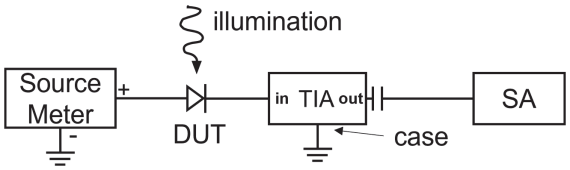

Fig. 3. Block diagram of the noise measurement setup.

setup. Essentially, a Keithley 2400 SourceMeter is used to provide a DC bias, and a Femto DLCPA-200 trans-impedance amplifier (TIA) is used to amplify the measured device noise so that it can be measured by an Agilent E4440A spectrum analyzer (SA). This measurement setup was used instead of a more conventional noise figure analyzer (NFA) based configuration because the desired measurement frequency is well below the minimum frequency of common NFAs like the Agilent 8973 NFA with a minimum frequency of 10 MHz. More details about this setup are described in a previous publication [13]. The TIA is set to the low-noise performance range with a trans-impedance of 10^5 V/A. The SA is centered at 69.4 kHz with a resolution bandwidth of 47 Hz. This specific measurement frequency was selected since the system noise floor was low enough to detect the generated noise from the measured device. For reference, the system noise floor was −116.1 dBm, and the low-measured noise power for both control structures was −114.9 dBm.

4. MEASURED EXCESS NOISE FOR STAIRCASE APDs

For all measurements, a bias of −2.5 V was used for the two-step staircase and its control, and a bias of −4 V was used for the three-step staircase and its control. These biases yield the maximum gain in each of the staircase structures. By using the same bias for both the control and its staircase, we ensure the control has the same depletion characteristics as the staircase, resulting in a direct comparison of only the signal and noise performance. All devices were illuminated with 543 nm light from a He-Ne continuous-wave laser, and all measurements were performed at room temperature.

The shot noise powers for an APD and a PIN are shown in Eq. (6) and Eq. (7), respectively. These equations are similar to Eq. (1) except the system impedance, $R = 50\ \Omega$, and measurement bandwidth, $\Delta f = 47$ Hz, have been introduced:

$$N_{\mathrm{APD,shot}} = 2q\left(I_{\mathrm{photo}} + I_{\mathrm{dark}}\right) R\Delta f \langle M\rangle^2 F(M), \tag{6}$$

$$N_{\mathrm{PIN,shot}} = 2q\left(I_{\mathrm{photo}} + I_{\mathrm{dark}}\right) R\Delta f. \tag{7}$$

A. Measuring the Noise Power of the Control Structures

To measure the excess noise of the two- and three-step staircase APDs, the noise versus photocurrent was first measured for the corresponding control structure. The control structure is simply a PIN photodiode producing a unity gain and unity excess noise. By varying the incident light intensity, and thus the photocurrent, a noise power of the control structures was measured corresponding to $2q(I_{\mathrm{photo}} + I_{\mathrm{dark}})R\Delta f + N_{\mathrm{system}}$. When plotting the measured noise versus photocurrent, there is a y-intercept at zero photocurrent corresponding to the dark noise contributions and any system noise. By subtracting the intercept, we are left with a line that scales linearly with photocurrent and represents $2q\,I_{\mathrm{photo}}\,R\Delta f$. These are the control photo lines in Figs. 4(a) and 4(b).

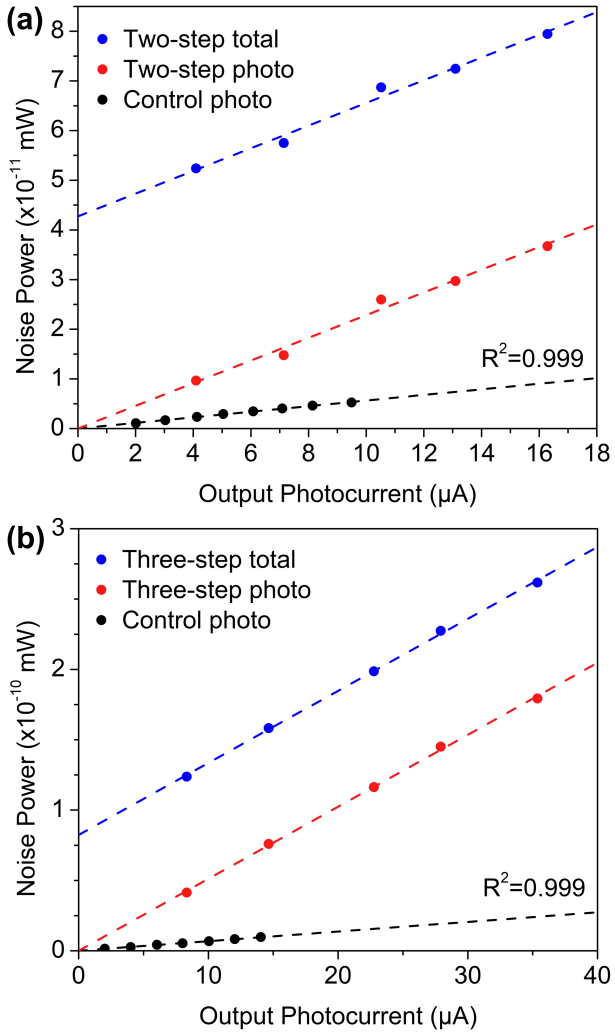

Fig. 4. (a) Measured noise power for a two-step staircase APD and its control. (b) Measured noise power for a three-step staircase APD and its control.

B. Measuring the Noise Power of the Staircase Structures

A similar measurement was performed for the staircase APD. With the staircase APD biased to achieve maximum output photocurrent, the device was illuminated with the same intensities exposed to the control. The staircase APD gain is its measured output photocurrent divided by the photocurrent of its control under the same illumination. The noise power was also measured at each intensity and corresponds to $2q(I_{\mathrm{photo}} + I_{\mathrm{dark}})R\Delta f\langle M\rangle^2 F(M) + N_{\mathrm{system}}$, the "$n$-step total" line in Figs. 4(a) and 4(b). The intercept of the "n-step total" line corresponds to the dark noise of the staircase APD and any system noise contributions. By subtracting the intercept, we get the "n-step photo" lines in Figs. 4(a) and 4(b), which are the photo noise power of the staircase devices corresponding to $2q\,I_{\mathrm{photo}}\,R\Delta f\langle M\rangle^2 F(M)$.

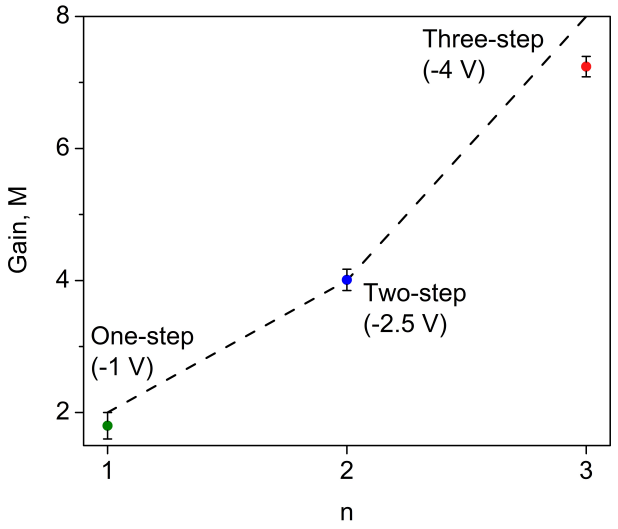

Fig. 5. Theoretical, 2^n, gain and measured gain for a one- [15], two-, and three-step staircase APD. The bias required to reach the plotted gain is in parentheses.

C. Calculating the Excess Noise Factor of the Staircase Structures

At the same input light intensities, the measured control noise corresponds to $2qI_{\text{photo}}R\Delta f$, and the measured staircase APD noise corresponds to $2qI_{\text{photo}}R\Delta f\langle M\rangle^2 F(M)$. Therefore, the excess noise factor of the staircase APD can be calculated by dividing the measured noise of staircase APD by the measured noise of the control and the squared gain of the staircase APD, $F(M) = N_{\text{APD}}/N_{\text{control}}\langle M\rangle^2$. This method for determining $F(M)$ accounts for any uncertainties with system gain and bandwidth, as well as any noise contributions from the laser source [14]. Since the staircase APD noise is divided by the control noise, these uncertainties will cancel, and only the excess noise intrinsic to the staircase device will remain. This method is preferred for determining $F(M)$ compared to direct calculation with Eq. (7).

Four devices were measured for both the two- and three-step staircase structures, and their excess noise was averaged. The measured average excess noise factors for the two- and three-step staircase APDs are 1.02 and 1.08, respectively. The corresponding average gains for the two- and three-step staircases are 4.01 and 7.24. The gain for a previously reported one-step [15] and the gains for the two- and three-step staircase APDs are plotted with the theoretical 2^n gain in Fig. 5.

Figure 6(a) shows the measured excess noise compared to the theoretical scaling of the best-case $k = 0$ conventional APD based on the local field model [17]:

$$F(M) = k\langle M\rangle + (1-k)\left(2 - \frac{1}{\langle M\rangle}\right), \tag{8}$$

where k is the ratio between β, the hole impact ionization coefficient, and α, the electron impact ionization coefficient. Also plotted is the excess noise of a Si APD [16] and two best-case high-gain first-dynode PMTs with two and three dynodes. For both PMTs, the gain of the first dynode, A, is equal to 10, and the "degrees-of-freedom," D, is ∞ (the least noisy) [10]. These degrees-of-freedom describe the variability of secondary-emission efficiency across the dynode surface [10]. The measured excess noise of both devices is much lower than that of the best-case $k = 0$ conventional APD and both best-case PMTs. Figure 6(b) shows the measured excess noise compared to the theoretical excess noise of staircase APDs expressed in Eq. (5). Instead of plotting directly versus the probability, P, the average gain was first calculated from the expression $\langle M\rangle = (1+P)^n$ and used. There is excellent agreement between the theoretical and measured noise for the two- and three-step staircase APDs.

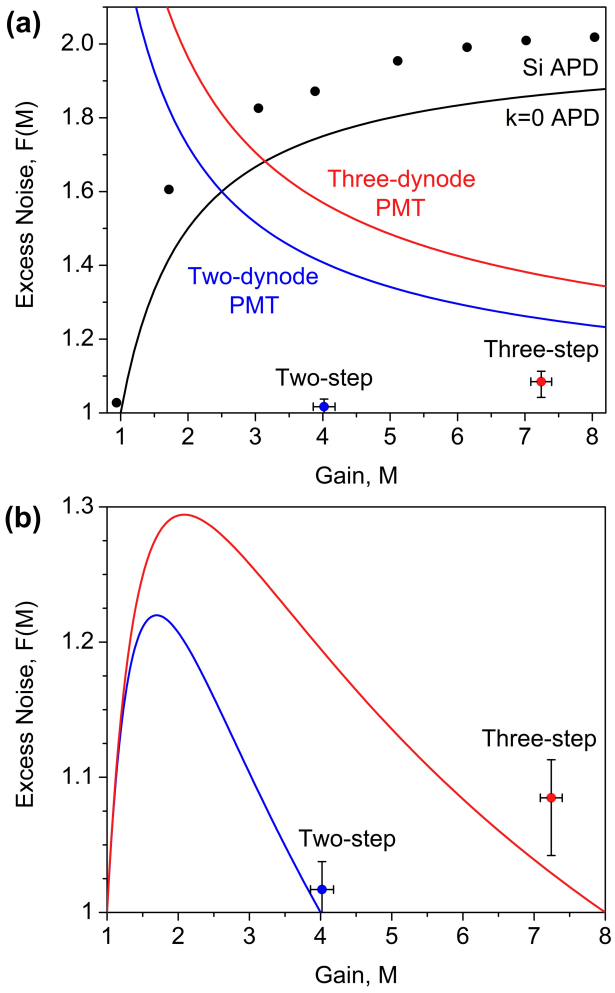

Fig. 6. (a) Measured excess noise factor for a two- and three-step staircase APD compared to the excess noise, based on Eq. (8), of a $k = 0$ conventional APD, a Si APD [16], and the theoretical excess noise of two best-case PMTs ($A = 10$, $D = \infty$) [10]. (b) Measured excess noise compared to the theoretical excess noise for a two- and three-step staircase APD.

5. CONCLUSION

We present excess noise measurements for both two- and three-step staircase APDs. The average gain for the two-step at −2.5 V is 4.01, with an average excess noise factor of 1.02. The average gain for the three-step at −4 V is 7.24, with an average excess noise factor of 1.08. Both values are much lower than the excess noise of a best-case $k = 0$ conventional APD. Additionally, the measured excess noise factors agree well with the original theoretical predictions made by Capasso *et al.* [1] and Teich *et al.* [10]. The near-unity excess noise factor of staircase APDs offers an exciting outlook on the potential future of high-sensitivity receiver systems.

Future iterations of this structure offer exciting implications for receiver sensitivities. First, due to the exponential gain scaling in staircase APDs, each additional staircase step added to the structure has the potential to double the gain. With the same near-unity excess noise factor, a future staircase APD design with four or five steps would provide double or quadruple the gain of a three-step device, while maintaining a receiver system that is still circuit noise limited. The main limitation, however, in realizing higher step count staircase APDs is ensuring that all the staircase steps unfold simultaneously. With each additional staircase step added, it becomes more difficult to balance the electrostatics of the device in a way to ensure all steps unfold together. If only some of the steps are unfolded, there could be significant charge trapping in the unfolded steps as they essentially act as an energy well. Additionally, suppose one step has completely unfolded and begins to flatten before the others. In that case, carriers may start to tunnel in the narrow bandgap region at the bottom of the step, resulting in increased dark currents. The addition of intermediate charge layers between steps may become necessary for higher step counts to ensure the proper step unfolding.

Additionally, for simplicity, the staircase APDs presented previously [7] and in this publication were grown with a relatively wide-bandgap absorber (∼1.2 eV). Future staircase APDs could incorporate a narrow bandgap material as the absorber in a separate absorption, charge, and multiplication structure where the conventional wide-bandgap multiplication region has been replaced with a staircase multiplication region, thus challenging the wavelength limitations of typical PMTs. Such a structure will be the subject of a future publication.

Funding. Defense Advanced Research Projects Agency (W909MY-12-D-0008, W911NF-17-1-0065); Army Research Office (W911NF-17-1-0065).

Disclosures. The authors declare no conflicts of interest.

Data availability. Data underlying the results presented in this paper may be obtained from the corresponding author upon reasonable request.

REFERENCES

1. F. Capasso, W.-T. Tsang, and G. F. Williams, "Staircase solid-state photomultipliers and avalanche photodiodes with enhanced ionization rates ratio," IEEE Trans. Electron Devices **30**, 381–390 (1983).
2. G. F. Williams, F. Capasso, and W. T. Tsang, "The graded bandgap multilayer avalanche photodiode: a new low-noise detector," IEEE Electron Device Lett. **3**, 71–73 (1982).
3. G. Ripamonti, F. Capasso, A. L. Hutchinson, D. J. Muehlner, J. F. Walker, and R. J. Malik, "Realization of a staircase photodiode: towards a solid-state photomultiplier," Nucl. Instrum. Methods Phys. Res. A **288**, 99–103 (1990).
4. I. K. Czajkowski, J. Allam, and A. R. Adams, "Role of satellite valleys in ionisation rate enhancement in multiple quantum well avalanche photodiodes," Electron. Lett. **26**, 1311–1313 (1990).
5. S. J. Maddox, S. D. March, and S. R. Bank, "Broadly tunable AlInAsSb digital alloys grown on GaSb," Cryst. Growth Des. **16**, 3582–3586 (2016).
6. J. Zheng, A. H. Jones, Y. Tan, A. K. Rockwell, S. March, S. Z. Ahmed, C. A. Dukes, A. W. Ghosh, S. R. Bank, and J. C. Campbell, "Characterization of band offsets in $Al_xIn_{1-x}As_ySb_{1-y}$ alloys with varying Al composition," Appl. Phys. Lett. **115**, 122105 (2019).
7. S. D. March, A. H. Jones, J. C. Campbell, and S. R. Bank, "Multistep staircase avalanche photodiodes with extremely low noise and deterministic amplification," Nat. Photonics **15**, 468–474 (2021).
8. L. G. Vaughn, L. Ralph, H. Xu, Y. Jiang, and L. F. Lester, "Characterization of AlInAsSb and AlGaInAsSb MBE-grown digital alloys," MRS Online Proc. Lib. **744**, M7.2 (2002).
9. H. S. Mączko, J. Kopaczek, S. J. Maddox, A. K. Rockwell, S. D. March, M. Gladysiewicz, S. R. Bank, and R. Kudrawiec, "An AlInAsSb/GaSb superlattice analysis–the digital alloy iduced conduction band states," in *International Conference on Numerical Simulation of Optoelectronic Devices (NUSOD)* (2018), pp. 45–46.
10. M. Teich, K. Matsuo, and B. Saleh, "Excess noise factors for conventional and superlattice avalanche photodiodes and photomultiplier tubes," IEEE J. Quantum Electron. **22**, 1184–1193 (1986).
11. K. M. Van Vliet and L. M. Rucker, "Noise associated with reduction, multiplication and branching processes," Phys. Stat. Mech. Appl. **95**, 117–140 (1979).
12. A. Pilotto, P. Palestri, L. Selmi, M. Antonelli, F. Arfelli, G. Biasiol, G. Cautero, F. Driussi, R. H. Menk, C. Nichetti, and T. Steinhartova, "A new expression for the gain-noise relation of single-carrier avalanche photodiodes with arbitrary staircase multiplication regions," IEEE Trans. Electron Devices **66**, 1810–1814 (2019).
13. A. A. Dadey, J. A. McArthur, A. H. Jones, S. R. Bank, and J. C. Campbell, "Considerations for excess noise measurements of low-k-factor Sb-based avalanche photodiodes," J. Opt. Soc. Am. A **40**, 1225–1230 (2023).
14. G. E. Bulman, V. M. Robbins, and G. E. Stillman, "The determination of impact ionization coefficients in (100) gallium arsenide using avalanche noise and photocurrent multiplication measurements," IEEE Trans. Electron Devices **32**, 2454–2466 (1985).
15. M. Ren, S. Maddox, Y. Chen, M. Woodson, J. C. Campbell, and S. Bank, "AlInAsSb/GaSb staircase avalanche photodiode," Appl. Phys. Lett. **108**, 081101 (2016).
16. M. E. Woodson, M. Ren, S. J. Maddox, Y. Chen, S. R. Bank, and J. C. Campbell, "Low-noise AlInAsSb avalanche photodiode," Appl. Phys. Lett. **108**, 081102 (2016).
17. R. J. McIntyre, "Multiplication noise in uniform avalanche diodes," IEEE Trans. Electron Devices **ED-13**, 164–168 (1966).